Prediction of Water Chemistry throughout the PWR Secondary System

Hyeeun Jeong [a], Jia Yu [b], Young-Jin Oh [b], Chi Bum Bahn [a*]
[a] *School of Mechanical Engineering, Pusan National University, Busan, Republic of Korea*
[b] *Power Engineering Research Institute, KEPCO Engineering&Construction, Gimcheon-si, Republic of Korea*
[*] *Corresponding author: bahn@pusan.ac.kr*

Keywords : secondary-side water chemistry, liquid-vapor partitioning, conductivity

1. Introduction

In the secondary system of pressurized water reactors (PWRs), thermal hydraulic variations – such as changes in pressure, temperature, and steam quality – govern the phase distribution of volatile species. These changes influence chemical concentrations and high-temperature pH in wet steam regions, thereby impacting corrosion and overall structural integrity. To maintain optimal water chemistry, pH control agents like ammonia (NH_3) and ethanolamine (ETA) are employed alongside hydrazine (N_2H_4) as a reducing agent [1].

Although various computational models exist to evaluate high-temperature pH and chemistry, most remain proprietary and restricted, impeding plant-specific application. Consequently, chemistry predictions for Korean PWRs often diverge from field observations due to simplified assumptions regarding species transport and thermal decomposition.

Building on a previous study [2] that developed a calculation code for the steam generator, the present study extends the code to the entire secondary system, integrating mass balance and phase equilibrium to represent flow, temperature, and volatility. It covers the main agents (NH_3, ETA, N_2H_4), ionic impurities (Na^+, Cl^-, SO_4^{2-}), and the organic acids (acetate, formate, glycolate) formed by ETA decomposition. For each condition, the code calculates pH_T and $pH_{25°C}$, and species concentrations. It also determines total conductivity (TC) and cation conductivity (CC) throughout the full secondary circuit, providing a practical tool for water chemistry management in nuclear power plants.

2. Calculation Methods

2.1 System Description

The secondary system is modeled as a series of components connected along the steam and water flow path, based on an APR1400 configuration [2] shown in Fig. 1. The main steam generated in the steam generator (SG) expands through the high-pressure turbine, passes through the moisture separator/reheater (MSR), and then expands through the low-pressure turbine before being condensed in the condenser. The condensate is then returned to the SG through the feedwater train, including feedwater heaters (FWH) and deaerator (DEA).

Each component is treated as a control volume with inlet and outlet streams, in which the liquid and vapor phases are handled separately. The chemistry within a component is determined by its temperature and steam quality, and the inlet concentrations. The outlet of each component thus defines the inlet condition of the next, so that the chemistry is propagated sequentially around the full secondary circuit.

Within this framework, the water chemistry conditions are evaluated at the key locations of each component, such as the SG blowdown (BD) and main steam (MS), the turbine extraction (EX) line, the MSR drain, condenser (CD) hotwell, DEA, and the FWH drain and tube side. The governing reactions and equations applied to every component are described in Sections 2.2 and 2.3.

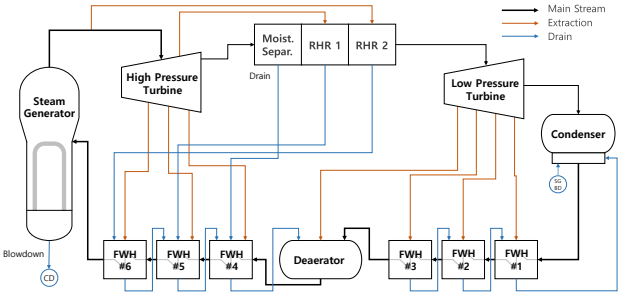


Fig 1. Schematic of APR1400 [3]

2.2 Chemical Reactions

Within each component, two classes of reactions are considered: ionization in the liquid phase and liquid-vapor partitioning.

Water self-ionizes, and each dissolved species dissociates according to its acid-base character [4]. Volatile amines act as weak bases and organic acids as weak acids, while the neutral forms associated with the ionic impurities (e.g., NaOH, HCl, $NaHSO_4$) participate in dissociation equilibria:

$$H_2O \overset{K_w}{\rightleftharpoons} H^+ + OH^- \quad (1)$$

$$B + H_2O \overset{K_{b,i}}{\rightleftharpoons} BH^+ + OH^- \quad (2)$$

$$HA \overset{K_{a,i}}{\rightleftharpoons} H^+ + A^- \quad (3)$$

Each volatile species i, including the neutral molecular forms such as HCl, also partitions between the liquid and vapor phases:

$$X_i(aq) \overset{K_{D,i}}{\rightleftharpoons} X_i(g) \quad (4)$$

2.3 Governing Equations

For every species, the system is closed by four relations: liquid-phase dissociation equilibria, species mass balance across each component, liquid-vapor partitioning through distribution coefficients, and charge conservation. The detailed formulation of these relations is given in a previous study [2], and is here generalized and applied to each component of the secondary system, extended to include the ionic impurities and the organic acids.

Combining these relations yields a set of nonlinear equations, which are linearized into the form Ax=b and solved iteratively, updating the hydrogen-ion concentration and ionic strength until convergence.

From the converged concentrations, the pH_T and $pH_{25°C}$ are obtained, and the total conductivity is evaluated from the ionic concentrations and their conductivities at 25 °C:

$$\kappa = \sum_i \lambda_i |z_i| C_i \quad (5)$$

where κ is the solution conductivity, λ_i is the conductivity of ion i at 25 °C [5], z_i is its charge number, and C_i is its molal concentration. The cation conductivity is the conductivity measured after the cations are exchanged for H^+, which removes the contribution of the alkalizing agents and enhances sensitivity to trace anionic impurities. It is computed by re-solving the equilibrium for the resulting acidified solution and applying Eq. (5).

3. Results

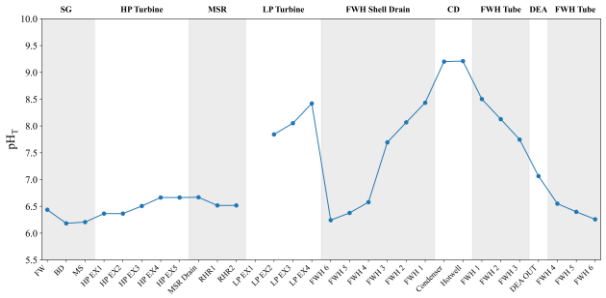
The calculation was performed under full-power operating conditions of the APR1400 secondary system. Thermal-hydraulic parameters for each component, such as temperature and flow rate, were specified based on plant design data. The feedwater concentrations were based on literature values [6] instead of actual operating conditions. Thermal decomposition of the ETA at SG was excluded in the present calculation, and the organic acids were instead specified directly at the feedwater as listed in Table I. Vent flow was also not considered here, although the model can account for venting at the CD, DEA, and FWH shell side.

Table I: Feedwater concentrations of the species [6]

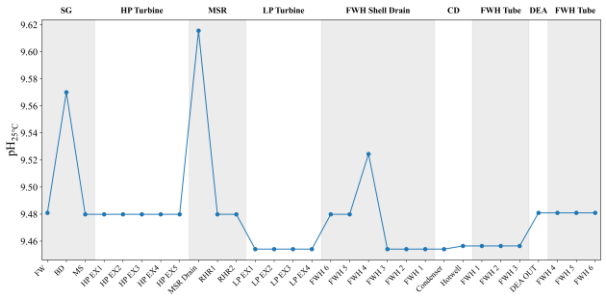
Species	Value (ppb)	Species	Value (ppb)
N_2H_4	92.41	SO_4^{2-}	0.006
ETA	1600	Acetate	11.11
NH_3	800	Formate	1.752
Na^+	0.034	Glycolate	0.07
Cl^-	0.313		

Fig. 2 shows the calculated water chemistry along the secondary system. The pH_T generally follows the temperature distribution. It is near 6.2 – 6.7 in the high-temperature region from the SG through the turbines, and rises above 9 in the condenser as the temperature approaches room temperature. The pH_T is not defined in the superheated-steam region between the MSR and the LP turbine because no liquid phase is present. The pH at 25 °C remains near 9.48 over most of the circuit. It increases at the SG blowdown and the MSR drain, where the injected chemicals concentrate in the retained liquid.

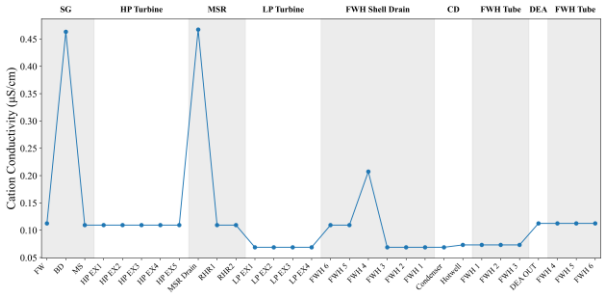
The cation conductivity shows a similar tendency, peaking at the SG blowdown and the MSR drain and staying low at the other locations. These peaks reflect the accumulation of impurities and organic acids in the liquid phase as volatile species preferentially partition into the vapor. They identify the locations most sensitive to impurity buildup along the secondary system.



(a) pH_T



(b) $pH_{25°C}$



(c) Cation Conductivity

Fig. 2. Calculated water chemistry along the secondary system

4. Conclusion and Future Work

In this study, the previously developed model was extended into a calculation code covering the entire PWR secondary system. It incorporates ionic impurities and organic acids, and computes the cation conductivity along with pH_T and $pH_{25°C}$. The code applied to the APR1400 predicts the location-dependent water chemistry by capturing the effects of phase partitioning and impurity concentration. It thus serves as a useful framework for water chemistry management. Future work will apply the model to transient conditions to predict the water chemistry under time-dependent operation.

ACKNOWLEDGEMENTS

This research was supported by the Korea Institute of Energy Technology Evaluation and Planning (KETEP) and the Ministry of Climate, Energy & Environment (MCEE) of the Republic of Korea (NO. RS-2022-KP002852 and NO. RS-2024-00398425).

REFERENCES

[1] Electric Power Research Institute, “PWR Advanced Amine Application Guidelines: Revision 2”, TR-102952-R2, EPRI, Palo Alto, CA, 1997.
[2] Jeong, Hyeeun, et al. "Thermodynamic modeling of secondary-side water chemistry in PWR steam generator." Nuclear Engineering and Technology, 2026.
[3] A.A. Alabbadi, and A.A. AlZahrani, “Nuclear hydrogen production using PEM electrolysis integrated with APR1400 power plant”, International Journal of Hydrogen Energy 60, 2024.
[4] J.W. Cobble, and P.J. Turner, “PWR Advanced All-Volatile Treatment Additives, By-Products, and Boric Acid”, TR-100755, EPRI, Palo Alto, CA, 1992.
[5] Haynes, William M., ed. “CRC handbook of chemistry and physics”, CRC press, 2016.
[6] Soonchunhyang University, Final Report on Development of Advanced Amine Chemistry Application Technology for Nuclear Power Plant Secondary System, Ministry of Knowledge Economy (MKE), Republic of Korea, 2011.